

The muon content of hybrid events recorded at the Pierre Auger Observatory

GLENNYS R. FARRAR¹ FOR THE PIERRE AUGER COLLABORATION²

¹Center for Cosmology and Particle Physics, Department of Physics, New York University, NY, NY 10003, USA

²Full author list: http://www.auger.org/archive/authors_2013_05.html
auger_spokespersons@fnal.gov

Abstract: The hybrid events of the Pierre Auger Observatory are used to test the leading, LHC-tuned, hadronic interaction models. For each of 411 well-reconstructed hybrid events collected at the Auger Observatory with energy $10^{18.8} - 10^{19.2}$ eV, simulated events with a matching longitudinal profile have been produced using QGSJET-II-04 and EPOS-LHC, for proton, He, N, and Fe primaries. The ground signals of simulated events have a factor 1.3-1.6 deficit of hadronically-produced muons relative to observed showers, depending on which high energy event generator is used, and whether the composition mix is chosen to reproduce the observed X_{\max} distribution or a pure proton composition is assumed. The analysis allows for a possible overall rescaling of the energy, which is found to lie within the systematic uncertainties.

Keywords: Pierre Auger Observatory, ultra-high energy cosmic rays, muons, hadronic interactions

1 Introduction

The ground-level muonic component of ultra-high energy (UHE) air showers is sensitive to hadronic particle interactions at all stages in the air shower cascade, and to many properties of hadronic interactions such as the multiplicity, elasticity, fraction of secondary pions which are neutral, and the baryon-to-pion ratio [1]. Air shower simulations rely upon hadronic event generators (HEGs), such as QGSJET-II [2], EPOS [3], and SIBYLL [4]. The HEGs are tuned on accelerator experiments, but when applied to air showers they must be extrapolated to energies inaccessible to accelerators and to phase-space regions not well-covered by existing accelerator experiments. These extrapolations result in a large spread in the predictions of the various HEGs for the muon production in air showers [5].

The hybrid nature of the Pierre Auger Observatory, combining both fluorescence telescopes (FD) [6] and surface detector array (SD) [7], provides an ideal experimental setup for testing and constraining models of high-energy hadronic interactions. Thousands of air showers have been collected which have a reconstructed energy estimator in both the SD and FD. The measurement of the longitudinal profile (LP) constrains the shower development and thus the signal predicted for the SD, at the individual event level.

2 Production of Simulated Events

In the present study, we compare the observed ground signal of individual hybrid events to the ground signal of simulated showers with matching LPs.

The data we use for this study are the 411 hybrid events with $10^{18.8} < E < 10^{19.2}$ eV recorded between 1 January 2004 and 31 December 2012 and satisfying the event quality selection cuts in [8, 9]. This energy range is sufficient to have adequate statistics while being small enough that the primary cosmic ray mass composition does not evolve significantly. For each event in this data set we generate Monte Carlo (MC) simulated events with a matching LP, as follows:

- Generate a set of showers with the same geometry and energy, until 12 of them have an X_{\max} value within one

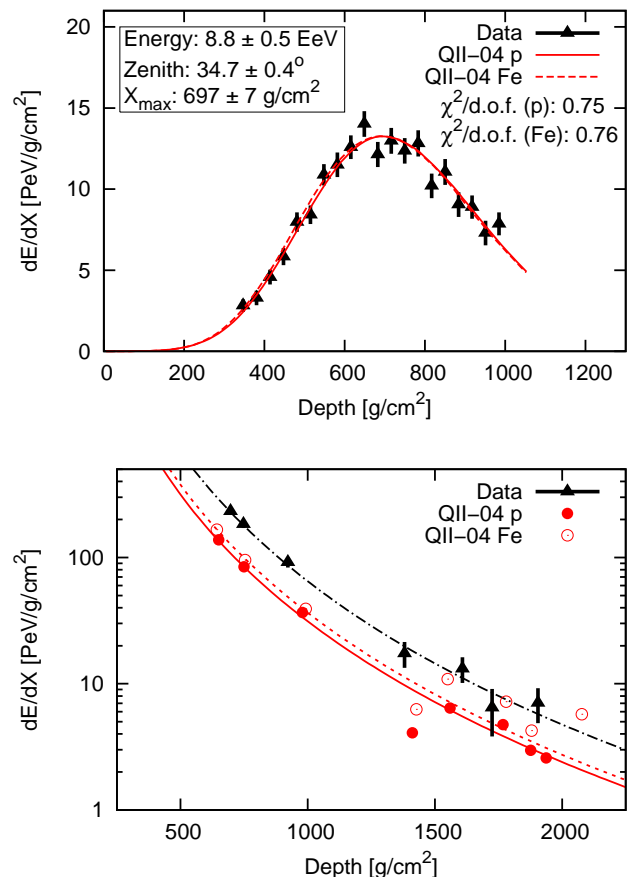


Figure 1: Top: The measured longitudinal profile of a typical air shower with two of its matching simulated air showers, for a proton and an iron primary, simulated using QGSJET-II-04. Bottom: The observed and simulated ground signals for the same event.

sigma of the real event.

- Among those 12 generated showers select, based on the χ^2 -fit, the 3 which best reproduce the observed longitudinal profile (LP).
- For each of those 3 showers do a full detector simulation

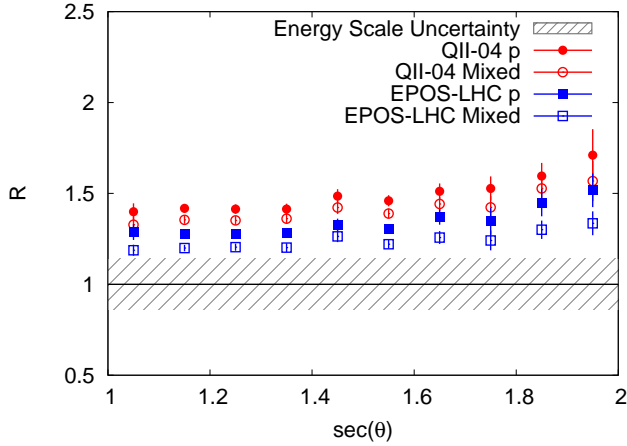


Figure 2: The average ratio of the $S(1000)$ of observed events to that in simulated events as a function of zenith angle for mixed or pure proton composition. The gray band represents the impact of the 14% systematic uncertainty in the FD energy scale.

and generate SD signals for comparison with the data.

We do this for two different HEGs (QGSJET-II-04 [10] and EPOS-LHC [11]) and for four different primary cosmic ray types (proton, helium, nitrogen, and iron) for all of the events in the dataset. Note, however, that in some events the X_{\max} value is so deep or shallow that the event cannot be reproduced with all four primaries in both HEGs.

Simulation of the detector response is performed with GEANT4 [12] within the software framework `Offline` [13] of the Auger Observatory. The MC air shower simulations are performed using the SENECA simulation code [14], with FLUKA [15, 16] as the low-energy HEG. Having three simulated showers which match the LP is sufficient to estimate the mean ground signal for the given LP.

The LP and lateral distribution of the ground signal of a typical event are shown in Fig. 1, along with a matching proton and iron simulated event. A high quality fit to the LP is found for all events for at least one primary type, and the χ^2 distribution of the selected LPs compared to the data is comparable to that found in a Gaisser-Hillas fit to the data.

Fig. 1 illustrates a general feature of the comparison between observed and simulated events: the ground signal of the simulated events is systematically smaller than the ground signal in the data events. Contributing factors to such a discrepancy in the ground signal could be a systematic energy offset, arising due to the 14% systematic uncertainty in the FD energy scale [8], or deficiencies in the HEGs. Elucidating the nature of the discrepancy is the motivation for the present study.

The estimated signal size at 1000 m, $S(1000)$, is the SD energy estimator. Fig. 2 shows the ratio of the $S(1000)$ of observed and simulated events for several HEGs, using a mixed composition that reproduces the X_{\max} distribution (Fig. 3), and also using pure protons for comparison. The discrepancy between measured and simulated $S(1000)$ grows with zenith angle for each HEG and is larger than the uncertainty in the FD energy scale at all angles. The growth of the discrepancy with zenith angle suggests that the simulations are predicting too few muons.

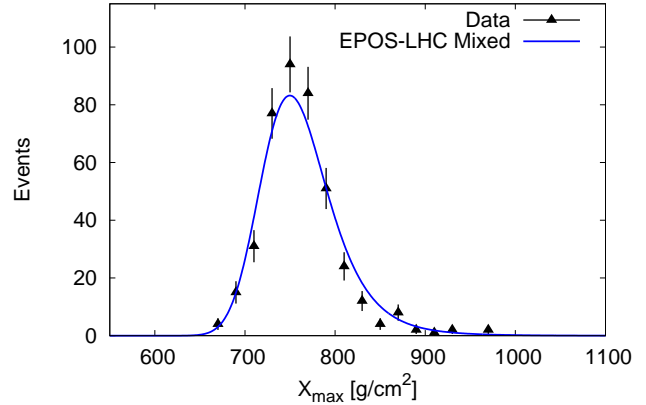


Figure 3: The X_{\max} distribution of the events used for this study, with the predicted shape from the best-fit $p_j(X_{\max})$ functions, for EPOS-LHC.

3 Quantifying the Discrepancy

To explore the potential sources of the discrepancy, the ground signal is modified in the simulated events to fit the ground signal in the data. Two rescaling factors are introduced: R_E and R_μ . R_E acts as a rescaling of the energy of the primary cosmic ray, which rescales the total ground signal of the event uniformly. R_μ acts as a ‘‘muonic’’ rescaling factor; it rescales only the contribution to the ground signal of inherently hadronic origin. For each event in the dataset, a rescaled simulated $S(1000)$ is calculated as a function of R_E , R_μ , and primary particle type. R_E and R_μ are then fit to minimize the discrepancy between the ensemble of simulated and observed $S(1000)$, for each HEG considered. The likelihood function to be maximized is $\prod_i P_i$, where the contribution of each event is

$$P_i = \sum_j p_j(X_{\max,i}) \mathcal{N}(S_{\text{resc}}(R_E, R_\mu)_{i,j} - S(1000)_i, \sigma_{i,j}).$$

The index i runs over each event in the data set and j labels the primary type; the factor $p_j(X_{\max,i})$ is the probability that the i th event comes from primary type j , given the X_{\max} of the event. We calculate $p_j(X_{\max})$ using the mix of p , He, N and Fe which best-fits the observed X_{\max} distribution, for each HEG. Determination of $\sigma_{i,j}$ and $S_{\text{resc}}(R_E, R_\mu)_{i,j}$ are discussed below.

The first step in determining $S_{\text{resc}}(R_E, R_\mu)_{i,j}$ is to attribute the ground signal of each simulated particle in the detector to either an electromagnetic (EM) or hadronic origin. To do this, the history of all muons and EM particles (e^\pm and γ s) reaching ground are tracked during simulation following the description in [17]. EM particles that are produced by muons, through decay or radiative processes, and by low-energy π^0 s are attributed to the muonic signal; muons that are produced through photoproduction are attributed to the electromagnetic signal. Fig. 4 shows the signal produced by each component of a 10 EeV air shower.

Because $S(1000)$ is a reconstructed property of each event, the impact of altering the muonic component or overall energy must be determined using reconstructed showers. To do this, we recalculate the detector response for each simulated shower, increasing the weight of the muonic component by the scale factors $w_\mu = 1.0, 1.75,$ and 2.5 , and a linear fit is performed to extract the EM and muonic components S_{EM} and S_μ via $S(1000)(w_\mu) \equiv S_{\text{EM}} + w_\mu S_\mu$. The rescaled simulated $S(1000)$ is then

$$S_{\text{resc}}(R_E, R_\mu)_{i,j} \equiv R_E S_{\text{EM},i,j} + R_E^\alpha R_\mu S_{\mu,i,j}, \quad (1)$$

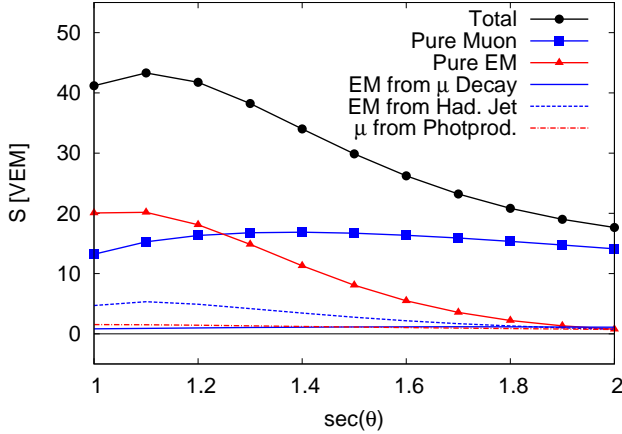


Figure 4: The contributions of different components to the average signal as a function of zenith angle, for stations at 1 km from the shower core, in simulated 10 EeV proton air showers illustrated for QGSJET-II-04. The signal size is measured in units of vertical equivalent muons (VEM), the calibrated unit of SD signal size [18].

where α is the energy scaling of the muonic signal; it has the value 0.89 in both the EPOS and QGSJET-II simulations, independent of composition [19].

Finally, the variance of $S(1000)$ with respect to S_{resc} must be estimated for each event. Contributions to the variance are of two types: the intrinsic shower-to-shower variance in the ground signal for a given LP, σ_{shwr} , and the variance due to limitations in reconstructing and simulating the shower, σ_{rec} and σ_{sim} . The total variance for event i and primary type j , is $\sigma_{i,j}^2 = \sigma_{\text{rec},i}^2 + \sigma_{\text{sim},i,j}^2 + \sigma_{\text{shwr},i,j}^2$.

σ_{shwr} is the variance in the ground signals of showers with matching LPs. This arises due to shower-to-shower fluctuations in the shower development which result in varying amounts of energy being transferred to the EM and hadronic shower components, even for showers with fixed X_{max} and energy. σ_{shwr} is irreducible, as it is independent from the detector resolution and statistics of the simulated showers. It is determined by calculating the variance in the ground signals of the simulated events from their respective means, for each primary type and HEG; it is typically $\approx 16\%$ of S_{resc} for proton initiated showers and 5% for iron initiated showers.

σ_{rec} contains i) the uncertainty in the reconstruction of $S(1000)$, ii) the uncertainty in S_{resc} due to the uncertainty in the calorimetric energy measurement, and iii) the uncertainty in S_{resc} due to the uncertainty in X_{max} ; σ_{rec} is typically 12% of S_{resc} . σ_{sim} contains the uncertainty in S_{resc} due to the uncertainty in S_{μ} and S_{EM} from the $S(1000) - w_{\mu}$ fit and to the limited statistics from having only three simulated events; σ_{sim} is typically 10% of S_{resc} for proton initiated showers and 4% for iron initiated showers.

The resultant model of $\sigma_{i,j}$ is checked using the 59 events, of the 411, which are observed with two FD eyes whose individual reconstructions pass all required selection cuts for this analysis. The variance in the S_{resc} of each eye is compared to the model for the ensemble of events. All the contributions to $\sigma_{i,j}$ are present in this comparison except for σ_{shwr} and the uncertainty in the reconstructed $S(1000)$. The variance of S_{resc} in multi-eye events is well represented by the estimated uncertainties using the model. In addition, the maximum-likelihood fit is also performed where σ_{shwr} is a free parameter rather than taken from the

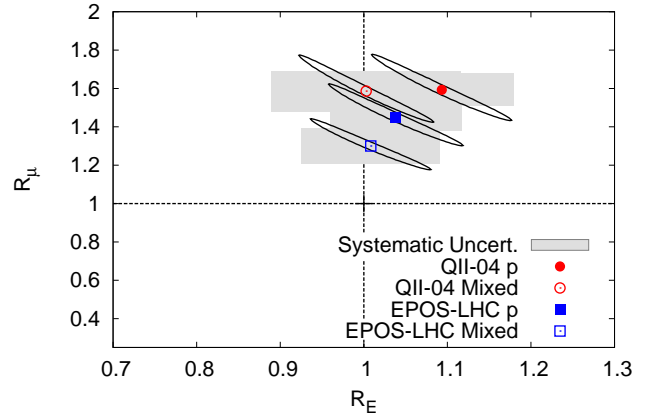


Figure 5: The best-fit values of R_E and R_{μ} for QGSJET-II-04 and EPOS-LHC, for mixed and pure proton compositions. The ellipses show the one-sigma statistical uncertainties. The grey boxes show the estimated systematic uncertainties as described in the text; these will be refined in a forthcoming journal paper.

models; no significant difference is found between the value of σ_{shwr} from the models, and that recovered when it is a fit parameter.

The results of the fit for R_E and R_{μ} are shown in Fig. 5 and Table 1 for each HEG. The ellipses show the one-sigma statistical uncertainty region in the $R_E - R_{\mu}$ plane. The systematic uncertainties in the event reconstruction of X_{max} , E_{FD} and $S(1000)$ are propagated through the analysis by shifting the reconstructed central values by their one-sigma systematic uncertainties; this is shown by the grey rectangles.¹ As a benchmark, the results for a purely protonic composition are given as well.²

The signal deficit is smallest (the best-fit R_{μ} is the closest to unity) in the mixed composition case with EPOS. As shown in Fig. 6, the primary difference between the ground signals predicted by the two models is the size of the muonic signal, which is ≈ 15 (20)% larger for EPOS-LHC than QGSJET-II-04, in the pure proton (mixed composition) cases respectively. EPOS benefits more than QGSJET-II when using a mixed composition because the mean primary mass determined from the X_{max} data is larger in EPOS than in QGSJET-II [20].

4 Discussion and Summary

In this work, we have used hybrid showers of the Pierre Auger Observatory to quantify the disparity between state-of-the-art hadronic interaction modeling and observed atmospheric air showers of UHECRs. The most important advance with respect to earlier versions of this analysis[21], in addition to now having a much larger hybrid dataset and improved shower reconstruction, is the extension of the anal-

1. The values of σ_{sim} , σ_{rec} and σ_{shwr} and the treatment of systematic errors used here will be refined with higher statistics Monte Carlo simulations and using the updated Auger energy and X_{max} uncertainties, for the journal version of this analysis.
2. Respecting the observed X_{max} distribution is essential for evaluating shower modeling discrepancies, since atmospheric attenuation depends on the distance-to-ground. This is automatic in the present analysis, but the simulated LPs – which are selected to match hybrid events – is a biased subset of all simulated events for a pure proton composition since with these HEGs pure proton does not give the observed X_{max} distribution.

Table 1: R_E and R_μ with statistical and systematic uncertainties, for QGSJET-II-04 and EPOS-LHC.

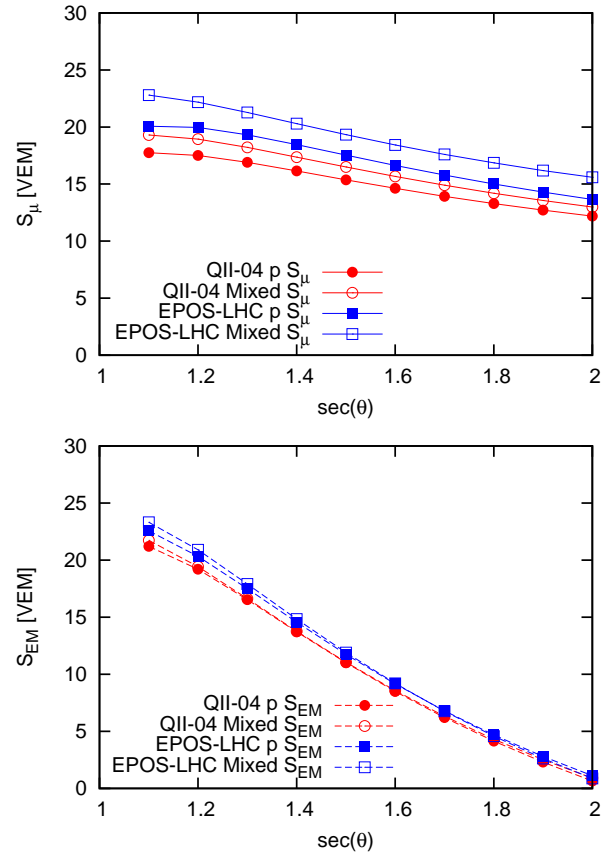
Model	R_E	R_μ
QII-04 p	$1.09 \pm 0.08 \pm 0.09$	$1.59 \pm 0.17 \pm 0.09$
QII-04 Mixed	$1.00 \pm 0.08 \pm 0.11$	$1.59 \pm 0.18 \pm 0.11$
EPOS p	$1.04 \pm 0.08 \pm 0.08$	$1.45 \pm 0.16 \pm 0.08$
EPOS Mixed	$1.01 \pm 0.07 \pm 0.08$	$1.30 \pm 0.13 \pm 0.09$

ysis method to treat a mixed composition that reproduces the X_{\max} distribution of the data. The previous analysis was restricted to a pure composition, which is inconsistent with the X_{\max} distribution predicted by these same hadronic interaction models. The pure-proton ansatz exaggerates the problem and the pure-Fe ansatz underestimates it.

To give the most basic characterization of the model discrepancies, our analysis introduces only a simple, overall rescaling of the hadronic shower relative to the EM shower, plus a possible overall energy recalibration (which proves not to be needed). In this context, the contributions to the muonic signal due to the hadronic and EM components of the showers can be distinguished, and our R_μ is the rescaling of the hadronic shower relative to the EM shower. As such, it is not directly comparable to direct muon number determinations provided by Pierre Auger Observatory, obtained from the FADC traces of the surface detector stations and from inclined showers (for which the ground signal is entirely muonic) [23, 24, 25, 26]. The direct methods report a purely experimental observable – the ground signal in muons, for showers in some zenith angle range – whereas R_μ characterizes the hadronic component of the showers. Nonetheless, all methods indicate that present shower models do not correctly describe the muonic ground signal; the general consistency of the methods is not surprising, since hadronic production is the prime source of muons.

Within the statistics currently available, there is no evidence of a larger event-to-event variance in the ground signal for fixed X_{\max} than predicted by the current models. This means that the muon shortfall cannot be attributed to some exotic phenomenon which produces a very large muon signal in only a fraction of events, such as micro-black hole production.

In summary, the observed hadronic signal in 10 EeV air showers ($E_{\text{CM}} = 137$ TeV) is a factor 1.3 to 1.6 larger than predicted using the leading hadronic interaction models tuned to fit LHC and lower energy accelerator data. Relative to the preliminary version of this analysis presented at ICRC2011[21], the central value of R_μ is closer to one and, with mixed composition, neither HEG calls for an energy rescaling. However the discrepancy between models and observation remains serious because i) the HEGs are now tuned to the LHC, ii) the analysis now allows for a mixed primary composition and has a more sophisticated treatment of fluctuations, and iii) the Auger event reconstruction and energy calibration have been refined[8]. With more than two times as many events, the discrepancy is twice the estimated systematic and statistical uncertainties combined in quadrature, even for the best case of EPOS-LHC with mixed composition.

**Figure 6:** Muonic (top) and EM signals (below) at 1000 meters as a function of zenith angle, in the models.

References

- [1] R. Ulrich *et al.*, Phys. Rev. D **83** (2011) 054026.
- [2] S. Ostapchenko, Nucl. Phys. B Proc. Supp. **151** (2006) 143.
- [3] K. Werner *et al.*, Phys. Rev. C **74** (2006) 044902.
- [4] E.-J. Ahn *et al.*, Phys. Rev. D **80** (2009) 094003.
- [5] R. Engel, D. Heck, and T. Pierog, Annu. Rev. Nucl. Part. Sci. **61** (2011) 467.
- [6] The Pierre Auger Collaboration, Nucl. Instrum. Methods A **620** (2010) 227.
- [7] The Pierre Auger Collaboration, Nucl. Instrum. Methods A **523** (2004) 50.
- [8] V. Verzi, for the Pierre Auger Collaboration, paper 0928, these proceedings.
- [9] R. Pesce, for the Pierre Auger Collaboration, Proc. 32nd ICRC, Beijing, China, **2** (2011) 214
- [10] S. Ostapchenko, Phys. Rev. D **38** (2011) 014018.
- [11] T. Pierog *et al.*, arxiv:1306.0121.
- [12] J. Allison *et al.*, IEEE Trans. Nucl. Sci. **53** (2006) 270.
- [13] S. Argirò *et al.*, Nucl. Instrum. Methods A **580** (2007) 1485.
- [14] H.-J. Drescher and G. Farrar, Phys. Rev. D **67** (2003) 116001.
- [15] G. Battistoni *et al.*, AIP Conf. Proc. **896** (2007) 31.
- [16] A. Ferrari *et al.*, CERN (2005).
- [17] M. Ave *et al.*, Proc. 32nd ICRC, Beijing, China, **2** (2011) 178.
- [18] X. Bertou *et al.*, Nucl. Instrum. Meth. A **568** (2006) 839.
- [19] J. Alvarez-Muñiz *et al.*, Phys. Rev. D **66** (2002) 033011.
- [20] The Pierre Auger Collaboration, JCAP **2** (2013) 026.
- [21] J. Allen, for the Pierre Auger Collaboration, Proc. 32nd ICRC, Beijing, China, **2** (2011) 83
- [22] J. Allen and G. Farrar, paper 1182, these proceedings.
- [23] A. Castellina, for the Pierre Auger Collaboration, Proc. 31st ICRC, Łódź, Poland (2009)
- [24] G. Rodríguez, for the Pierre Auger Collaboration, Proc. 32nd ICRC, Beijing, China, **2** (2011) 95
- [25] B. Kégl, for the Pierre Auger Collaboration, paper 0860, these proceedings.
- [26] I. Valiño, for the Pierre Auger Collaboration, paper 0635, these proceedings.